

# Photocalorimetric Studies of Singlet Oxygen Reactions

John Olmsted III

Contribution from the Chemistry Department, California State University, Fullerton, Fullerton, California 92634. Received July 6, 1979

**Abstract:** The technique of photomicrocalorimetry has been used to determine photochemical quantum yields and reaction enthalpies for tetraphenylporphine (TPP)-sensitized photooxygenation of several singlet oxygen acceptors. It is shown that, under favorable conditions (reactive acceptor, long singlet oxygen lifetime), the quantum yield of photooxygenation is equal to the triplet yield of sensitizer (0.88 for TPP in CCl<sub>4</sub>). For less reactive acceptors and/or in solvents in which the singlet oxygen lifetime is short, reaction quantum yields are acceptor concentration dependent but have upper concentration limits equal to the sensitizer triplet yield, demonstrating that physical (as opposed to reactive) quenching of singlet oxygen by reactive acceptors does not occur. Reaction enthalpies for photooxygenation are as follows (kJ/mol, all in CCl<sub>4</sub> solvent): 1,3-diphenylisobenzofuran, -205; 2,5-dimethylfuran, -95; 2,3-dimethyl-2-butene, -185; 1,3-cyclohexadiene, -175; 9,10-diphenylanthracene, -55.

The techniques of calorimetry have not been much utilized in studying photochemical reactions. Pioneering efforts by Magee and Daniels around 1940 demonstrated that calorimetry could be used both to determine the overall enthalpy change associated with photochemical reactions<sup>1</sup> and to study photochemical quantum yields,<sup>2</sup> but, as their apparatus was elaborate and lacking in long-term stability, the technique was not pursued further. Much more recently, Seybold, Gouterman, and Callis demonstrated that calorimetry could also be used to measure fluorescence quantum yields.<sup>3</sup> Calorimetric studies of photochemical systems became much more feasible with the advent of thermistor temperature sensors. Within the past 3 years, we have demonstrated the utility of thermistor-sensor apparatus for fluorescence quantum yields determinations<sup>4,5</sup> and for photon flux measurements,<sup>6</sup> and several groups have been developing the technique to determine overall reaction enthalpy changes.<sup>7,8</sup>

What has not been hitherto recognized is that calorimetric measurements, as the early experiments of Magee and Daniels suggested, can provide important information not only about photochemical energetics but also about the quantum yields of the reacting system. We demonstrate in this paper that it is possible, *using calorimetric monitoring only*, to extract values for the triplet quantum yield of a sensitizer and for the overall photoreaction quantum yield.

The photochemical system which we have used in this work is dye-sensitized photooxygenation of organic molecules. Such photooxygenation reactions involving singlet oxygen have been extensively studied, yet there remain aspects of these reactions about which there is some uncertainty. Enthalpy changes accompanying photooxygenation have not been determined to date, although Stevens has found discrepancies between estimated standard formation enthalpies and activation energy data for the 9,10-diphenylanthracene-singlet oxygen system.<sup>9</sup>

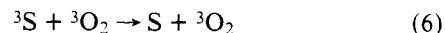
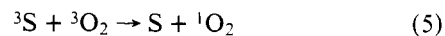
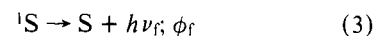
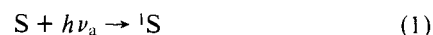
Physical quenching of singlet oxygen by potentially reactive substrates has been occasionally observed<sup>10,11</sup> and was suggested by Matheson et al. to be possibly a general phenomenon.<sup>12</sup> Data for some substrates, however, have been shown to be incompatible with the existence of physical quenching.<sup>13,14</sup> Although it is clear that physical quenching occurs in certain instances (e.g., sulfides), the prevalence of such quenching of singlet oxygen by reactive substrates remains in doubt, and the seeming inconsistencies in the data reported for the very reactive acceptor 1,3-diphenylisobenzofuran (DPBF) have yet to be resolved.

In hopes of contributing to the resolution of these uncertainties, as well as of demonstrating the general utility of the photocalorimetric technique, we have examined the calorimetry of the dye-sensitized photooxygenation of various sub-

strates in several different solvents. The results of these studies are reported in this paper.

## Theory

We consider the following set of reactions to encompass the processes occurring in sensitized photochemical oxygenation:



Under conditions of our experiments, the sensitizer S is present in sufficiently high concentration to absorb all (>99%) of the incident monochromatic radiation. This results in an energy input to the system:

$$(dE/dt)_{in} = h\nu_a(dn/dt) \quad (11)$$

where  $dn/dt$  is the incident photon flux. When the sensitizer has an appreciable fluorescence quantum yield, a portion of this energy input is released as emitted photons:

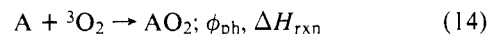
$$(dE/dt)_{\Pi} = h\nu_f\phi_f(dn/dt) \quad (12)$$

In the absence of acceptor A, the overall effect of the other primary processes is the degradation of the energy input into heat:

$$(dE/dt)_{heat} = (dn/dt)(h\nu_a - \phi_f h\nu_f) = C(dT_r/dt) \quad (13)$$

where C represents the total heat capacity of the system and the temperature rise under these conditions is designated  $dT_r$ .

When a suitable singlet oxygen acceptor is added to the system, the occurrence of the oxygenation reaction (reaction 9) introduces an additional energy term owing to the enthalpy change in the overall reaction



The energy appearing as heat is now given by the equation

$$(dE/dt)_{\text{heat}} = (dn/dt)(h\nu_a - \phi_f h\nu_f - \phi_{\text{ph}} \Delta H_{\text{rxn}}/N_0) = C(dT_a/dt) \quad (15)$$

where Avogadro's number  $N_0$  is included to convert the reaction enthalpy from a molar to a molecular basis and  $\phi_{\text{ph}}$  is the photochemical quantum yield of the photooxygenation reaction.

If eq 13 and 15 are rearranged and the appropriate combination taken, eq 16 results:

$$\frac{(dT_r/dt) - (dT_a/dt)}{(dT_r/dt)} = \phi_{\text{ph}} \Delta H_{\text{rxn}}/N_0(h\nu_a - \phi_f h\nu_f) \quad (16)$$

When sensitizer fluorescence is negligible and heating rates are measured over short, equal time intervals, the equation can be further simplified:

$$(\Delta T_r - \Delta T_a)/\Delta T_r = \phi_{\text{ph}} \Delta H_{\text{rxn}}/N_0 h\nu_a \quad (17)$$

Equation 17 allows the determination of  $\phi_{\text{ph}} \Delta H_{\text{rxn}}$  from measurements of the temperature change of the system in the presence and absence of acceptor.

The photochemical quantum yield of a reaction having a satisfactorily large enthalpy change can also be determined calorimetrically. If the system is irradiated for a time long enough to destroy completely the acceptor, the resulting total energy change is

$$\Delta E_a = n(h\nu_a - \phi_f h\nu_f) - \Delta H_{\text{rxn}} m = C \Delta T_a \quad (18)$$

where  $m$  is the number of moles of acceptor initially present,  $n$  is the total number of photons absorbed, and  $\Delta T_a$  is the total temperature rise during irradiation. If the solution without acceptor is irradiated for an identical time, its resulting energy change is

$$\Delta E_r = n(h\nu_a - \phi_f h\nu_f) = C \Delta T_r \quad (19)$$

the symbols having similar meanings. The difference between these two equations gives

$$\Delta T_a - \Delta T_r = -\Delta H_{\text{rxn}} m/C \quad (20)$$

On the other hand, the difference between eq 13 and 15 gives

$$dT_a/dt - dT_r/dt = \phi_{\text{ph}} \Delta H_{\text{rxn}} (dn/dt)/N_0 C \quad (21)$$

Dividing eq 21 by eq 20 yields

$$\frac{dT_a/dt - dT_r/dt}{\Delta T_a - \Delta T_r} = \frac{\phi_{\text{ph}} dn/dt}{N_0 m} \quad (22)$$

Thus knowledge of the total excess heating due to presence of acceptor, photon flux, number of moles of acceptor, and instantaneous heating rate allows computation of the instantaneous photochemical quantum yield.

When the acceptor reaction rate is very rapid and the unimolecular decay rate of singlet oxygen is slow, the quantum yield and heating rates will be independent of acceptor concentration so long as acceptor remains present. In that case, eq 22 can be simplified:

$$\phi_{\text{ph}} = \frac{mN_0}{t} \frac{dn/dt}{dn/dt} \left[ \frac{dT_a/dt - dT_r/dt}{\Delta T_a/t - \Delta T_r/t} \right] = \frac{mN_0}{t} \frac{dn/dt}{dn/dt} = mN_0/n \quad (23)$$

In other words, when  $\phi_{\text{ph}}$  is concentration independent, it is given simply by the number of molecules of acceptor divided by the number of photons needed to consume the acceptor.

Calorimetric determination of these quantum yields requires independent knowledge of the photon flux rate  $dn/dt$ . As we have previously shown, this can also be determined calorimetrically if an electrical source providing calibrated energy input

is part of the system.<sup>6</sup> Hence, a suitable photometric calorimeter having a means of monitoring temperature rise, a transparent window permitting illumination, and an electrical heating coil can be utilized to determine enthalpy changes and quantum yields accompanying sensitized photochemical reactions.

The photochemical quantum yield for disappearance of acceptor in a reaction system described by eq 1-10 can be expressed in terms of yields of various intermediates, which can in turn be related to reaction rate constants. Assuming that no more than one acceptor molecule is consumed upon reaction with singlet oxygen, the yield of product from singlet oxygen is

$$\gamma \text{AO}_2 = k_9[A]/(k_8 + k_9[A] + k_{10}[A]) \quad (24)$$

Similarly, the yield of singlet oxygen from triplet sensitizer is

$$\gamma^1 \text{O}_2 = k_5[{}^3\text{O}_2]/(k_7 + k_5[{}^3\text{O}_2] + k_6[{}^3\text{O}_2]) \quad (25)$$

The quantum yield of triplet sensitizer depends on the rates of unimolecular decay of the excited singlet sensitizer:

$$\phi_t = k_2/(k_2 + k_3 + k_4) \quad (26)$$

Then the net quantum yield of acceptor disappearance, which is the same as the net yield of product, is the product of these three factors:

$$\phi_{\text{ph}} = \phi_t \gamma^1 \text{O}_2 \gamma \text{AO}_2 \quad (27)$$

Physical quenching of triplets by oxygen ( $k_6$ ) is generally unimportant relative to energy-transfer quenching ( $k_5$ ), which for a variety of triplet molecules reaches its theoretical limit of ca.  $2 \times 10^9 \text{ M}^{-1} \text{ s}^{-1}$ .<sup>15</sup> Since oxygen-saturated solutions typically have oxygen concentrations around  $10^{-2} \text{ M}$ <sup>16</sup> and unimolecular triplet decay rates ( $k_7$ ) are typically  $\leq 10^4 \text{ s}^{-1}$ , the yield of singlet oxygen from sensitizer triplets,  $\gamma^1 \text{O}_2$ , will be effectively unity. The yield of product from singlet oxygen, on the other hand, may be unity for an efficiently reacting acceptor such as 1,3-diphenylisobenzofuran in a solvent such as  $\text{CCl}_4$  in which the singlet oxygen lifetime is long.<sup>7</sup> In other solvents, for other less reactive acceptors, or for acceptors which are capable of physical ( $k_{10}$ ) as well as reactive ( $k_9$ ) quenching,  $\gamma \text{AO}_2$  will depart from unity and the observed photochemical quantum yield will be less than the triplet yield of the sensitizer. When physical quenching is dominant, the product yield is concentration independent:

$$\gamma' \text{AO}_2 = k_9/(k_9 + k_{10}) \quad (28)$$

When unimolecular singlet oxygen decay is dominant, the product yield varies with concentration:

$$\gamma'' \text{AO}_2 = k_9[A]/(k_8 + k_9[A]) \quad (29)$$

Hence, analysis of the variation of  $\phi_{\text{ph}}$  with acceptor concentration together with comparison of  $\phi_{\text{ph}}$  and  $\phi_t$  allows an assessment of the importance of physical quenching. Furthermore, substitution of eq 29 into eq 27 and inversion yields

$$\phi_{\text{ph}}^{-1} = \phi_t^{-1}(1 + k_8/k_9[A]) \quad (30)$$

Thus, plots of reciprocal quantum yields vs. reciprocal concentration should be linear with slope/intercept ratios of  $k_8/k_9$ .

## Experimental Section

The photometric calorimetry apparatus was the same as has been described in detail.<sup>6</sup> Briefly, light from a 100-W Hg medium-pressure lamp (Illumination Industries 110 lamp in LH-371 housing) was passed through an interference filter (Baird-Atomic) and focused on the front window of a Dewar cell containing the solution to be studied. The Dewar cell was immersed in a room temperature water bath. A

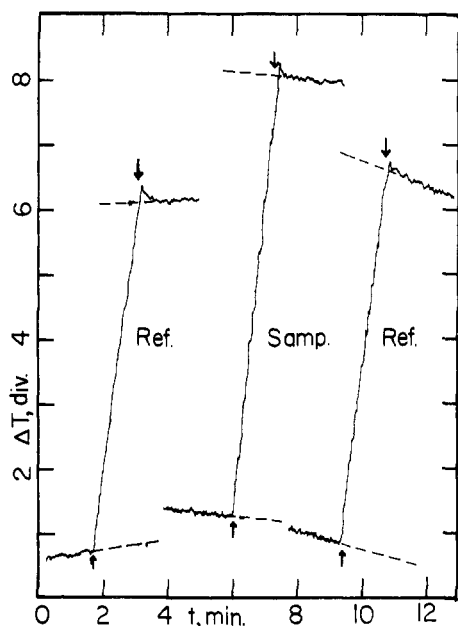


Figure 1. Representative photometric heating rates for short (1.5 min) irradiation times. Upward arrows designate onset of illumination, downward arrows termination of illumination. Temperature scale is in arbitrary units. Solution was 30 mL of  $\text{CCl}_4$  solvent containing *meso*-tetraphenylporphine sensitizer, illuminated at 546 nm. Left-hand reference tracing is before introduction of substrate, sample tracing is after introduction of 10  $\mu\text{L}$  of 2,3-dimethyl-2-butene (TME), and right-hand reference tracing is after complete consumption of TME.

Table I. Photocalorimetry of DPBF in  $\text{CCl}_4$ <sup>a</sup>

irradiation interval, min	amount of heating (chart divisions)	irradiation interval, min	amount of heating (chart divisions)
0-2	108.8	8-10	107.2
2-4	110.2	10-12	85.8 <sup>b</sup>
4-6	107.4	12-14	79.1
6-8	106.9	14-16	76.6

<sup>a</sup> Sensitizer, *meso*-tetraphenylporphine; irradiation wavelength, 546 nm;  $0.97 \times 10^{-4}$  mol of DPBF. <sup>b</sup> Change of slope observed at 10.5-min irradiation.

thermistor probe-Wheatstone bridge combination (Sargent S-81630 and S-81601) connected to a strip-chart recorder monitored the temperature change of the solution. For photon flux measurements, an electrical resistance heating coil was immersed in the solution and photometric and electrical heating rates were compared.<sup>6</sup> For photooxygenation studies, the heating coil was removed and oxygen, presaturated with solvent vapor by passage through two bubbling towers, was bubbled through the solution by means of a hypodermic needle.

Rates of heating of the systems being studied were determined for the following solution conditions; sensitizer only, without  $\text{O}_2$  bubbling; sensitizer only, with  $\text{O}_2$  bubbling; sensitizer and reactive substrate, with  $\text{O}_2$  bubbling; sensitizer and completely reacted substrate, with  $\text{O}_2$  bubbling; sensitizer only, electrical heating. In a typical run, 30 mL of solution containing sufficient sensitizer to give an optical density greater than 2 (3-cm solution depth) was introduced into the cell and allowed to equilibrate thermally. Photometric and electrical heating rates were then determined by alternately illuminating and electrically heating the system for timed periods of 1-3 min. The electrical heater was then removed, the hypodermic needle introduced, and oxygen bubbling commenced. After reequilibration, additional photometric heating rates were obtained. A weighed (solid substrates) or volumetric (liquid substrates) quantity of singlet oxygen acceptor, of the order  $10^{-5}$  mol, was then introduced, following which photometric heating rates were determined for sequential 1.5- or 2-min exposures until the heating rate was once again the same as before introduction

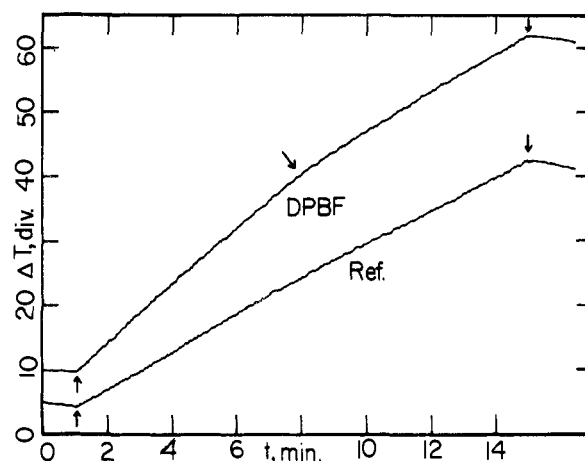


Figure 2. Representative photometric heating rates for long (14 min) irradiation times. Upward arrows designate onset of illumination, downward arrows termination of illumination. Temperature scale is in arbitrary units, but unit size is the same as in Figure 1. Diagonal arrow indicates time when DPBF substrate is completely consumed. Solution was 30 mL of  $\text{CCl}_4$  solvent containing *meso*-tetraphenylporphine sensitizer, illuminated at 546 nm. Reference tracing is before introduction of substrate; DPBF tracing is after introduction of 10 mg of 1,3-diphenylisobenzofuran (DPBF).

of the substrate. Representative recorder tracings of these heating rates are shown in Figure 1. The oxygen bubbler was then removed, the electrical heater was reintroduced, and photometric and electrical heatings were repeated once more.

The fluorescence quantum yield of the sensitizer was determined by comparison of the integrated emission spectra of sensitizer and of a suitable fluorescence standard,<sup>8</sup> at excitation wavelengths at which solution absorbances had been previously matched using a Cary 15 spectrophotometer. Fluorescence spectra were taken on an Aminco-Bowman spectrophotofluorimeter equipped with a red-sensitive photomultiplier tube.

The following chemicals were used as received from the supplier: 1,3-diphenylisobenzofuran, 9,10-diphenylanthracene, 2,5-dimethylfuran (Aldrich); 1,3-cyclohexadiene, 2,3-dimethyl-2-butene (Chemical Samples Co.); *meso*-tetraphenylporphine (Strem Chemicals); Freon 113 (Matheson). Carbon tetrachloride was spectrograde and toluene was reagent grade, fractionally distilled before use.

## Results

**I. 1,3-Diphenylisobenzofuran (DPBF).** Since DPBF is one of the most reactive singlet oxygen acceptors and singlet oxygen has a long lifetime in  $\text{CCl}_4$  solvent, initial experiments were done on this system. Figure 2 shows the heating rates of solutions of *meso*-tetraphenylporphine (TPP) sensitizer in  $\text{CCl}_4$ , irradiated at 546 nm, in the absence and presence of DPBF. The exothermicity of the reaction is evident, as is the change in slope at the time when DPBF is fully consumed. The slopes of the heating curves in Figure 2 are not fully linear, because, as the solution heats up, the rate of heat losses to the environment are increased. When a series of shorter irradiations was run, base-line corrections were made to compensate for this change (see Figure 1).

Heating-rate data for DPBF in  $\text{CCl}_4$  are given in Table I. The constancy of the heating rate over the first 10 min of irradiation is apparent. In this case eq 23 can be applied, giving  $\phi_{\text{ph}} = 0.875$ , and the reaction enthalpy is computed to be  $-205$  kJ/mol by means of eq 17.

For Freon 113 (1,1,2-trichlorotrifluoroethane) as solvent, sensitizer solubility was lower and consequently an excitation wavelength of 404 nm was used. At that wavelength, fluorescence from the DPBF was readily observed, even though optical densities were such that 95% of the incident light was absorbed by the sensitizer. The fluorescence allowed visual monitoring of the acceptor simultaneously with calorimetric

**Table II.** Calorimetric Results for Tetraphenylporphine-Sensitized Photooxygenations<sup>a</sup>

substrate	solvent	$\phi_{\text{reaction}}^b$ ( $\pm 0.03$ )	$\Delta H_{\text{reaction}}$ , kJ/ mol ( $\pm 20$ kJ)
DMF <sup>c</sup>	CCl <sub>4</sub>	0.90	-95
DPBF <sup>d</sup>	CCl <sub>4</sub>	0.88	-205
TME <sup>e</sup>	CCl <sub>4</sub>	0.87	-185
CHD <sup>f</sup>	CCl <sub>4</sub>	<i>h</i>	-175
DPA <sup>g</sup>	CCl <sub>4</sub>	<i>h</i>	-55
DPBF	toluene	0.88	-185
TME	toluene	<i>h</i>	-160
DPBF	Freon 113 <sup>i</sup>	1.00	-195
TME	Freon 113 <sup>i</sup>	0.98	-175

<sup>a</sup> 546-nm excitation except where noted. <sup>b</sup> Lower limit of sensitizer triplet yield. <sup>c</sup> 2,5-Dimethylfuran. <sup>d</sup> 1,3-Diphenylisobenzofuran. <sup>e</sup> 2,3-Dimethyl-2-butene (tetramethylethylene). <sup>f</sup> 1,3-Cyclohexadiene. <sup>g</sup> 9,10-Diphenylanthracene. <sup>h</sup> Concentration dependent; see Figure 3. <sup>i</sup> 404-nm excitation.

determinations, and it was observed that acceptor fluorescence disappeared simultaneously with the change of slope of the solution heating curve, directly verifying that the calorimetric method is an accurate assay of acceptor consumption. Freon 113 is also a solvent in which singlet oxygen has a long lifetime;<sup>12</sup> thus, the quantum yield of photoreaction is effectively constant and the data are analyzed using eq 23 and 17, with results given in Table II.

The lifetime of singlet oxygen in toluene is substantially shorter than in halogenated hydrocarbons (see below); in toluene, nonetheless, the reaction quantum yield for DPBF was found to be concentration independent above concentrations of  $1.6 \times 10^{-3}$  M. This limiting quantum yield and the overall reaction enthalpy are given in Table II.

**II. 2,3-Dimethyl-2-butene (TME).** 2,3-Dimethyl-2-butene (tetramethylethylene) is a somewhat less reactive acceptor for singlet oxygen;<sup>17</sup> in both CCl<sub>4</sub> and Freon 113 it nonetheless reacts with an essentially concentration-independent quantum yield at concentrations above  $4 \times 10^{-4}$  M. In toluene, on the other hand, the reaction quantum yield is distinctly concentration dependent even above  $10^{-3}$  M. A plot of reciprocal yield vs. reciprocal concentration, shown in Figure 3, is reasonably linear. From its slope-intercept ratio, using the Merkel and Kearns value of  $4 \times 10^7 \text{ M}^{-1} \text{ s}^{-1}$  for acceptor reaction rate constant, a lifetime of singlet oxygen of 23  $\mu\text{s}$  in toluene was obtained. Quantum yields and reaction enthalpies for TME in all three solvents are given in Table II.

The TME disappearance rate could also be followed conveniently using NMR, since the single reactant resonance at 1.65 ppm gives way to a series of resonances including one at 1.2 ppm. When the reaction quantum yield was calculated from the integrated peak areas of these two peaks at various irradiation times, the value so obtained for CCl<sub>4</sub> solution was 0.86, identical with the value obtained using the calorimetric technique.

**III. Other Acceptors.** The enthalpies and quantum yields of three other singlet oxygen acceptors were determined in CCl<sub>4</sub> solution and are included in Table II. One of these, 2,5-dimethylfuran (DMF), is nearly as reactive toward singlet oxygen as is DPBF.<sup>17</sup> For DMF, NMR analysis was also carried out and gave a quantum yield of 0.88 compared to 0.91 from calorimetric data. For this acceptor as for DPBF the photochemical quantum yield was essentially concentration independent.

1,3-Cyclohexadiene (CHD) is a substantially poorer singlet oxygen acceptor, for which the photochemical quantum yield even in CCl<sub>4</sub> shows substantial concentration dependence. A reciprocal quantum yield vs. reciprocal concentration plot is shown in Figure 3, from whose slope/intercept ratio, using the

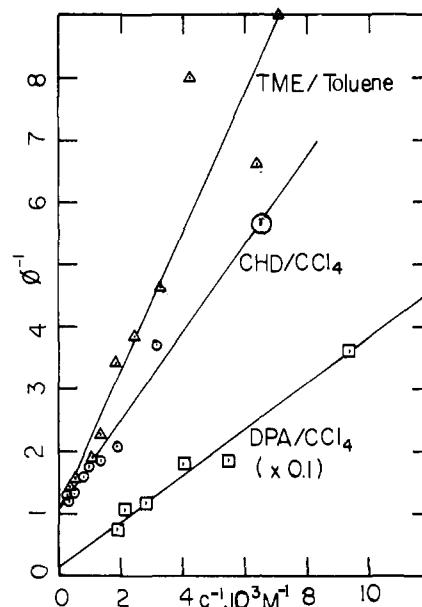


**Figure 3.** Plots of reciprocal photochemical quantum yields vs. reciprocal substrate concentration. Reciprocal quantum yields reduced tenfold for DPA/CCl<sub>4</sub> system. TME, 2,3-dimethyl-2-butene; CHD, 1,3-cyclohexadiene; DPA, 9,10-diphenylanthracene.

Merkel and Kearns value of 700  $\mu\text{s}$  for the singlet oxygen lifetime in CCl<sub>4</sub>,<sup>17</sup> a reaction rate constant of  $1.8 \times 10^6 \text{ M}^{-1} \text{ s}^{-1}$  is computed. CHD is thus some 20 times less reactive than TME and 400 times less reactive than DPBF. Foote found CHD to be 12.5 times less reactive than TME;<sup>18</sup> since that value is based on a single determination, the agreement appears to be satisfactory.

Finally, the reaction of 9,10-diphenylanthracene (DPA) with singlet oxygen was examined. For this acceptor, the reaction enthalpy and quantum yields are too small for the calorimetric method to be utilized alone, but the quantum yields (which are concentration dependent) can be assayed by monitoring the rate of disappearance of the DPA absorption peak at 376 nm, where sensitizer absorption is relatively low. These data are also shown on the reciprocal plot of Figure 3, and from that plot the reaction rate constant for DPA is found to be  $6 \times 10^5 \text{ M}^{-1} \text{ s}^{-1}$ .

## Discussion

**I. Sensitizer Triplet Yield.** As shown in the Theory section, for a sufficiently reactive singlet oxygen acceptor the overall photoreaction quantum yield will be equal to the sensitizer triplet yield, whereas for less reactive acceptors the triplet yield is the upper limit for the photoreaction yield. From the values given in Table II, and from the concentration independence of those values for DPBF in all three solvents, the triplet yields of TPP are  $0.88 \pm 0.03$  in CCl<sub>4</sub> and in toluene and  $0.99 \pm 0.03$  in Freon 113. The yield of 0.88 in toluene is in excellent agreement with the value of  $0.82 \pm 0.12$  determined by Dzhagarov.<sup>19</sup>

Tetraphenylporphine is somewhat fluorescent in all three of these solvents, with an emission maximum at around 660 nm. The fluorescence quantum yield in toluene was measured both by a calorimetric technique<sup>4</sup> and by fluorimetric comparison with a violanthrone standard in toluene,<sup>20</sup> giving  $\phi_f = 0.05 \pm 0.02$ . Fluorimetric comparison against cresyl violet in ethanol<sup>20</sup> for TPP in Freon 113 gave  $\phi_f = 0.035 \pm 0.01$ . These fluorescence yields are consistent with the triplet yields and indicate that internal conversion is unimportant in Freon 113 and plays only a minor role in CCl<sub>4</sub> and toluene solvents.

**II. Physical Quenching of Singlet Oxygen.** The suggestion of Matheson et al.<sup>12</sup> that physical quenching of singlet oxygen

**Table III.** Singlet Oxygen Acceptor Parameters (CCl<sub>4</sub> Solvent)

acceptor <sup>a</sup>	rate constant, M <sup>-1</sup> s <sup>-1</sup>	limiting quantum yield
DPBF	8 × 10 <sup>8</sup> <sup>b</sup>	0.88 ± 0.03 <sup>d</sup>
DMF	4 × 10 <sup>8</sup> <sup>b</sup>	0.90 ± 0.03 <sup>d</sup>
TME	4 × 10 <sup>7</sup> <sup>b</sup>	0.86 ± 0.03 <sup>d</sup>
CHD	1.8 × 10 <sup>6</sup> <sup>c</sup>	0.87 ± 0.04 <sup>e</sup>
DPA	6 × 10 <sup>5</sup> <sup>c</sup>	0.83 ± 0.06 <sup>e</sup>

<sup>a</sup> See Table II for identification of compounds. <sup>b</sup> Reference 13. <sup>c</sup> This work. <sup>d</sup> Concentration independent. <sup>e</sup> Infinite-concentration limit.

may be a relatively general process in solution is not borne out by our results. On the contrary, there is no significant physical quenching for any of the substrates and solvents studied in this work. In toluene solution, this is demonstrated by the agreement of the photochemical quantum yield with the triplet yield for TPP. In Freon 113, the photochemical quantum yield of effectively 1.0 for both DPBF and TME acceptor rules out any nonreactive quenching. In CCl<sub>4</sub>, those photochemical quantum yields which were concentration independent are the same, indicating that, if physical quenching were occurring, it would have to be proportionately the same for all three acceptors. Moreover, the infinite-concentration limit for the quantum yields of those two acceptors which showed a concentration dependence (i.e., the y intercepts in Figure 3) are also the same as these concentration-independent yields. As Table III demonstrates, the upper limit to the photoreaction quantum yield is the same for acceptors having singlet oxygen reaction rates which vary over 1000-fold.

The case of 1,3-diphenylisobenzofuran requires further attention. Evans and Tucker pointed out that, if the reaction product is *o*-dibenzoylbenzene, only one oxygen atom is incorporated per acceptor, and thus the overall photochemical yield could be twice the singlet oxygen yield.<sup>21</sup> However, the work of Rio and Scholl<sup>22</sup> on the DPBF photooxide shows that, while the eventual thermal reactions may be complex, the initial photoproduct is the transannular peroxide, which is relatively stable. Our results bear this out in that the photochemical yield is the same for DPBF as for TME in all three solvents; one would expect different yields if more complex stoichiometry were involved. Hence, the direct determination reported here is in agreement with the analyses of Merkel and Kearns<sup>13</sup> and Foote and Ching<sup>14</sup> and the results of Evans and Tucker<sup>21</sup> that DPBF does not physically quench singlet oxygen in solution.

**III. 9,10-Diphenylanthracene.** The 9,10-diphenylanthracene molecule is of particular interest because of the thermal reversibility of the peroxidation reaction, which is capable of generating singlet oxygen virtually quantitatively.<sup>23</sup> Stevens and Small<sup>9</sup> studied the activation energy for the reversion reaction and found it to be probably inconsistent with reported formation enthalpies of DPA and its peroxide. Our value for the overall enthalpy change for the photochemical reaction agrees with measured formation enthalpies for anthracene and its peroxide<sup>24</sup> and is entirely consistent with the activation energy. Combining the reaction enthalpy of -55 kJ mol<sup>-1</sup> with the excitation energy of <sup>1</sup>Δ<sub>g</sub> oxygen of 93 kJ mol<sup>-1</sup> yields a predicted activation energy barrier for the reverse reaction of at least 148 kJ mol<sup>-1</sup>, whereas the measured values of Stevens and Small are 135 kJ mol<sup>-1</sup>. Given the experimental uncertainties, the two values are in agreement, indicating that the thermal regeneration reaction is the reverse of the acceptor addition reaction and that there is a very small or zero activation energy barrier for the reaction of singlet oxygen with DPA.

In view of this, one must inquire why the rate constant for the photooxygenation reaction is some 1000-fold slower for DPA than for DPBF. The most likely explanation would ap-

pear to be that the DPA-<sup>1</sup>O<sub>2</sub> collision complex undergoes extremely facile redissociation to starting material, such that only about 1 in 1000 collision complexes reacts before dissociating. This is consistent with the very efficient regeneration of singlet oxygen upon thermal decomposition of DPA peroxide and also with the fact that thermal decomposition does not appear to cause significant reoxidation of the DPA itself.

**IV. Reaction Enthalpies.** As the data in Table II demonstrate, the overall reaction enthalpy for the addition of oxygen to the substrates used in this study is consistently exothermic, and, within our quoted experimental error of ±20 kJ/mol, this enthalpy change is solvent independent at least for the nonpolar solvents used in this study.

Although enthalpy of formation data for butene hydroperoxides are not available, data are available for 2-methylpropane (-155 kJ/mol) and its peroxide analogue *tert*-butyl hydroperoxide (-294 kJ/mol),<sup>25</sup> from which an enthalpy of peroxidation of -140 kJ/mol would be predicted. Our measured value for TME is -175 kJ/mol, a substantially larger value. If the slight endothermicity (+ 8.4 kJ/mol) of the 2-butene to 1-butene shift accompanying the peroxidation is also taken into account, the discrepancy is some 40 kJ/mol, suggesting that the allylic hydroperoxide is significantly more stable than its alkyl analogue. A possible explanation for the higher exothermicity is formation of a hydrogen-bonded dimer by the hydroperoxide, but this is ruled out by the NMR spectrum of the photoproduct, which shows a sharp peak at 7.0 ppm, exactly where the *tert*-butyl hydroperoxide monomer peak falls and some 1 ppm downfield from the dimer peak.<sup>26</sup> A satisfactory explanation for the enhanced stability of the allylic hydroperoxide is not readily apparent.

Among the transannular peroxides, the significantly greater reaction enthalpy for 1,3-diphenylisobenzofuran (-205 kJ/mol) compared to 2,5-dimethylfuran (-95 kJ/mol) is readily accounted for by the resonance stabilization of the benzene ring that is formed when the isobenzofuran is bridged across the 1,3 positions. On the other hand, 1,3-cyclohexadiene also shows a relatively high reaction enthalpy (-175 kJ/mol) which cannot be so readily explained. There may be a stabilizing interaction between the π electrons of the double bond and the nonbonding electrons of the oxygen atoms, but we know of no independent evidence for such an occurrence.

**Acknowledgment** is made to the Research Corporation and to the donors of the Petroleum Research Fund, administered by the American Chemical Society, for support of this research.

## References and Notes

- (1) J. L. Magee and F. Daniels, *J. Am. Chem. Soc.*, **62**, 2825 (1940).
- (2) J. L. Magee, T. W. DeWitt, E. C. Smith, and F. Daniels, *J. Am. Chem. Soc.*, **61**, 3529 (1939).
- (3) P. G. Seybold, M. Gouterman, and J. Callis, *Photochem. Photobiol.*, **9**, 229 (1969).
- (4) M. Mardelli and J. Olmsted III, *J. Photochem.*, **7**, 277 (1977).
- (5) D. Magde, J. H. Brannon, T. L. Creemers, and J. Olmsted III, *J. Phys. Chem.*, **83**, 696 (1979).
- (6) J. Olmsted III, *Rev. Sci. Instrum.*, **50**, 1256 (1979).
- (7) G. Jones II, W. R. Bergmark, and T. E. Reinhardt, *Sol. Energy*, **20**, 241 (1978).
- (8) A. W. Adamson, A. Vogler, H. Kunkely, and R. Wachter, *J. Am. Chem. Soc.*, **100**, 1298 (1978).
- (9) B. Stevens and R. D. Small, Jr., *J. Phys. Chem.*, **81**, 1605 (1977).
- (10) W. S. Geason, A. D. Broadbent, E. Whittie, and J. N. Pitts, Jr., *J. Am. Chem. Soc.*, **92**, 2068 (1970).
- (11) C. S. Foote and J. W. Peters, *J. Am. Chem. Soc.*, **93**, 3795 (1971).
- (12) I. B. C. Matheson, J. Lee, B. S. Yamanashi, and M. L. Wolbarsht, *J. Am. Chem. Soc.*, **96**, 3343 (1974).
- (13) P. B. Merkel and D. R. Kearns, *J. Am. Chem. Soc.*, **97**, 462 (1975).
- (14) C. S. Foote and T.-Y. Ching, *J. Am. Chem. Soc.*, **97**, 6209 (1975).
- (15) D. R. Kearns, *Chem. Rev.*, **71**, 395 (1971).
- (16) Landolt-Börnstein, "Zahlenwerte und Funktionen," 6 Auflage, II Band, 2 Teil, Bandteil b, Springer-Verlag, West Berlin, 1962.
- (17) P. B. Merkel and D. R. Kearns, *J. Am. Chem. Soc.*, **94**, 7244 (1972).
- (18) C. S. Foote, *Acc. Chem. Res.*, **1**, 104 (1968).
- (19) B. M. Dzharogov, *Opt. Spectrosc. (Engl. Transl.)*, **28**, 33 (1970).
- (20) J. Olmsted III, *J. Phys. Chem.*, **83**, 2581 (1979).

- (21) D. F. Evans and J. N. Tucker, *J. Chem. Soc., Faraday Trans. 2*, **72**, 1661 (1976).  
 (22) G. Rio and M.-J. Scholl, *J. Chem. Soc., Chem. Commun.*, 474 (1975).  
 (23) H. H. Wassermann, J. R. Scheffer, and J. L. Cooper, *J. Am. Chem. Soc.*, **94**, 4991 (1972).  
 (24) P. Bender and J. Farber, *J. Am. Chem. Soc.*, **74**, 1450 (1952).  
 (25) D. R. Stull, E. F. Westrum, Jr., and G. C. Sinke, "The Chemical Thermodynamics of Organic Compounds," Wiley, New York, 1969.  
 (26) D. Severn, A. H. Clements, and T. M. Luong, *Anal. Chem.*, **41**, 412 (1969).

## Relative Rates and Kinetic Isotope Effects of Reactions in Solution

Joseph R. Murdoch

Contribution from the Department of Chemistry, University of California, Los Angeles, California 90024. Received February 3, 1978

**Abstract:** Recently, there has been considerable interest in relating curvature observed in rate-equilibrium relationships to "intrinsic" barriers for proton-transfer reactions. These results have attracted wide attention since many of the "intrinsic" barriers are surprisingly small and range between 1 and 5 kcal/mol. The overall rates of these reactions are far too slow to be accounted for by such small barriers, and it is necessary to assign the difference to an unusually large barrier for assembling the reactants together into a reactive configuration (i.e., an encounter step). The encounter step(s) may involve diffusion, solvent reorganization, orientation, or molecular distortions rather than bond formation which contributes to the "intrinsic" barrier. A fundamental implication of these results is that making and breaking chemical bonds is often *less* important than encounter as a contributor to the overall barrier.

Curvature can have an *intrinsic* component which is associated with changes in rate and equilibrium constants for the proton-transfer step, as well as a *coupling* component which arises from *coupling* of proton transfer with other steps in the overall reaction. It is the *intrinsic* contribution which is relevant for calculating "intrinsic" barriers, but in the past these two contributions have not been clearly delineated. In the present paper a relationship between the *intrinsic* and *coupling* components is derived. It is shown that variations in relative rates and kinetic isotope effects due to factors intrinsic to the proton transfer step cannot be easily distinguished from variations due to coupling of other steps with proton transfer. As a result, calculated "intrinsic" barriers can be too low by 75–100% for small barriers (e.g., 2 kcal) and by 5–13 kcal/mol, or more, for larger barriers (e.g., 25 kcal/mol). Corresponding errors in the opposite direction are introduced into the encounter contribution to the observed barrier. A significant point is that the *coupling* component of the curvature can be large enough to reverse the relative importance of bond formation and encounter as elements of the observed barrier.

### I. Curvature in Rate-Equilibrium Relationships

Rate-equilibrium relationships have been of interest ever since Brønsted,<sup>1</sup> Bell,<sup>2</sup> and Evans and Polanyi<sup>3</sup> suggested empirical relationships between the activation energy and the thermodynamics of an overall reaction:

$$\Delta G^\ddagger = \alpha' \Delta G^\circ + \beta'$$

$$\Delta E_a^\ddagger = \alpha'' \Delta H^\circ + \beta''$$

The parameter  $\alpha'$  provided a measure of the relative sensitivities of  $\Delta G^\ddagger$  and  $\Delta G^\circ$  to substituent effects and was frequently interpreted as an indicator of the structural similarity between the transition state and the reactants or products of the reaction.<sup>4</sup> For many years it was thought that endergonic reactions should show a larger dependence on  $\Delta G^\circ$  than exergonic reactions, so that reactions with negative values of  $\Delta G^\circ$  should be associated with lower values of  $\alpha'$  than reactions with positive  $\Delta G^\circ$ 's. This effect should give rise to curvature in plots of  $\log k$  vs.  $\Delta G^\circ$ , but for almost 40 years no one was able to demonstrate *unambiguously* the anticipated dependence of  $\alpha'$  on  $\Delta G^\circ$  until Eigen<sup>5a</sup> produced curved rate-equilibrium plots involving proton transfer between bases and acids containing O, N, and C.

Eigen<sup>5a</sup> and Ahrens and Maass<sup>6</sup> also showed that the curvature was significantly more pronounced for reaction series which had larger rate constants at  $\Delta G^\circ = 0$ , so that proton transfers between O and N gave sharply curved Brønsted plots, while proton transfer reactions involving carbon gave almost linear plots over extended regions of  $\Delta pK$ .<sup>5</sup> This led to the idea that curvature in rate-equilibrium plots and the rate constant

for the thermoneutral member of the reaction series were qualitatively related.

Since Eigen's original demonstration of curved rate-equilibrium relationships, numerous other examples of curvature have also appeared. These include proton-transfer reactions,<sup>7–16</sup> carbonyl additions,<sup>17,18</sup> nucleophilic attack,<sup>19</sup> radical-transfer reactions,<sup>20</sup> and fluorescence quenching by electron transfer.<sup>21,22</sup> to cite only a few examples. Observed curvature in rate-equilibrium relationships has been used to help choose between mechanistic alternatives<sup>16,19,21,22</sup> and to calculate "intrinsic" barriers for related series of reactions.<sup>7–15,17,18</sup> The "intrinsic" barrier is defined as the reaction barrier at  $\Delta G^\circ = 0$  and a "related series of reactions" is often defined as those reactions sharing a common "intrinsic" barrier. These relationships have frequently been expressed through Marcus' equation<sup>12</sup>

$$\Delta G^\ddagger = (\Delta G^\circ)^2 / 16\Delta G_0^\ddagger + \frac{1}{2}\Delta G^\circ + \Delta G_0^\ddagger \quad (1)$$

$$\alpha = \left( \frac{\partial \Delta G^\ddagger}{\partial \Delta G^\circ} \right)_{\Delta G_0^\ddagger, T, P}$$

where  $\Delta G^\circ$  is the free energy of reaction for an *elementary* step,  $\Delta G^\ddagger$  is the free energy of activation, and  $\Delta G_0^\ddagger$  is the "intrinsic" barrier for the reaction.

Since eq 1 is a parabolic relationship, a plot of  $\Delta G^\ddagger$  vs.  $\Delta G^\circ$  will show a degree of curvature which depends on the magnitude of  $\Delta G_0^\ddagger$ .<sup>12</sup> Recently, a number of authors<sup>7–21</sup> have made use of this fact in order to estimate intrinsic barriers for several classes of proton transfer and other types of reactions. Many of the intrinsic barriers are remarkably small, ranging in most